PROCEEDINGS OF SCIENCE

The Very High Energy Sky from ~ 20 GeV to Hundreds of TeV - Selected Highlights

Mathieu de Naurois*
LLR - IN2P3/CNRS - Ecole Polytechnique
E-mail: denauroi@in2p3.fr

arXiv:1510.00635v1 [astro-ph.HE] 2 Oct 2015

After nearly a decade of operation, the three major arrays of atmospheric Cherenkov telescopes have revolutionized our view of the Very High Energy Universe, unveiling more than 100 sources of various types. MAGIC, consisting of two 17 m diameter telescopes on the Canary island of La Palma, and VERITAS, with four 12 m telescopes installed in southern Arizona, USA, have primarily explored the extragalactic sky, where the majority of the sources are active galactic nuclei (AGN), with γ-ray emission originating in their relativistic jets. In July 2014 MAGIC discovered the most distant source of very high energy γ rays, the gravitationally lensed blazar S3 0218 residing at the redshift of $z = 0.944$. The flat spectrum radio quasar PKS 1441+25 ($z = 0.939$), observed by MAGIC & VERITAS in 2015, showed a strong flaring activity over a time span of several weeks. Rapid variability from various BL Lacertae objects, down to minute timescales, has been observed by the three experiments, and measurement of their high-energy spectra allows the level of extragalactic background light to be constrained.

Since the commissioning of the fifth, large (28 m diameter) telescope in December 2012, H.E.S.S.-II is the only array operating telescopes of different sizes together ("*hybrid array* "). The largest Cerenkov telescope ever built, CT5, provides an energy threshold of ~ 20 GeV. With its broad energy range, H.E.S.S. explored the Galactic Plane with unprecedented sensitivity. The legacy release of the H.E.S.S. Galactic Plane Survey, consisting of 2800 hours of observations of the Galactic disk, reveals major new results. This is the first high-resolution (~ 0.1 deg) sensitive ($\sim 2\%$ Crab Nebula point-source sensitivity) survey of the Milky Way in VHE γ rays.

The Milky Way harbors a large variety of high energy sources of various types. In recent years, deep observations of several key Galactic regions of utmost importance for this field have been conducted by the three experiments. Among them are the Galactic Center region and its halo (particularly relevant for dark matter searches), the Cygnus region and its mysterious Milagro sources, the Crab Nebula and pulsar (surprisingly showing pulsed emission up to above 1 TeV), the iconic γ-ray supernova remnant RX J1713.7-3946 and other SNRs such as Tycho, the Vela pulsar and several binary systems such as LS 5039, PSR B1259-63, HESS J0632+057 and LS I $+61^\circ$ 303. Joint observations on several of these objects proved to be the most efficient way to understand their nature. A deep observation of the Large Magellanic Cloud revealed, for the first time, spectacular and powerful accelerators of stellar origin outside our own galaxy.

Highlights of these observations with H.E.S.S., MAGIC and VERITAS have been presented and discussed at the conference.

The 34th International Cosmic Ray Conference,
30 July- 6 August, 2015
The Hague, The Netherlands

*Speaker.

© Copyright owned by the author(s) under the terms of the Creative Commons Attribution-NonCommercial-ShareAlike Licence.

Introduction

In the last years, the field of very high energy (VHE) γ-rayastronomy evolved in several directions, taking advantage of the improved sensitivities over time (see Fig. 1):

- Large surveys, consisting of several hundreds - or even thousands - of hours have been performed by the H.E.S.S. experiment in the central regions of the Galaxy and by the VERITAS collaboration in the Cygnus region. These surveys provide a unique way to characterize the VHE source population in a uniform, unbiased way, and open the way to population studies.

- Deep exposures have been taken on a handful of sources of particular importance ("*key science projects*"), allowing in-depth understanding of the acceleration and radiation mechanisms, but also constraining upper limits on exotic physics and dark matter searches. This has been made possible by the development of sophisticated analysis techniques and a much deeper understanding of the instruments.

- A particular effort has been undertaken to reduce the energy threshold of the instruments and bridge the gap to *Fermi*-LAT. The VERITAS collaboration [2] upgraded its telescopes with high quantum efficiency PMTs in 2012 [3] while MAGIC is since 2009 operating in stereo mode.

- The largest Imaging Atmospheric Cerenkov Telescope ever built, namely the fifth telescope of H.E.S.S.-II (CT5), has been inaugurated and is now operating regularly, allowing observations of γ rays down to $\sim$ 10 GeV. H.E.S.S. is currently performing a major upgrade of the Cerenkov telescopes 1 – 4 [4] in order to lower their threshold when operated with CT5 and reduce their dead-time.

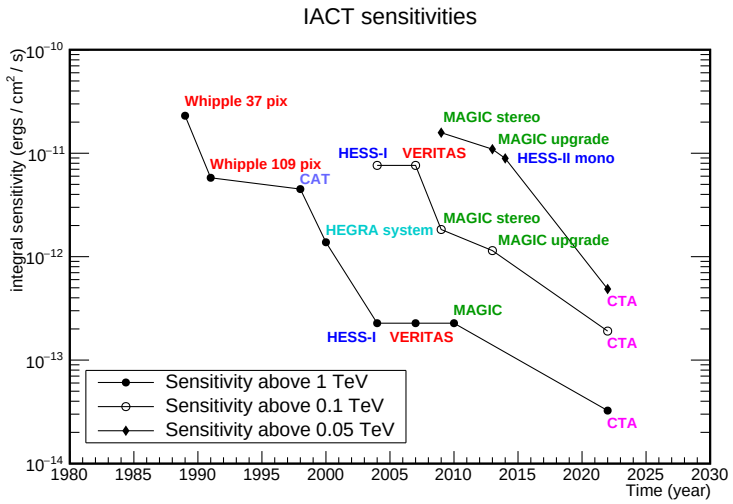

Figure 1: Evolution of integral sensitivity of the IACTs over time, above 50 GeV (filled diamonds), 100 GeV (open circles) and 1 TeV (filled circles) [1]. The expected sensitivities of CTA are also shown.

- After the success of Milago [5, 6], the High Altitude Water Cerenkov (HAWC) [7, 8], a large water Cerenkov detector with a very large field of view, has been inaugurated in March 2015. Very well suited to full-sky surveys, HAWC, has been the subject of a dedicated review talk [9] and is therefore not covered by this paper.

1. The H.E.S.S. Legacy Survey

The H.E.S.S. Galactic plane survey (HGPS) [13] was performed with the H.E.S.S.-I Cerenkov telescope array in Namibia from 2004 to 2013. After several publications on a small ($\sim 10\%$) fraction of the current data set [14, 15], it is the deepest and most comprehensive, high resolution (~ 0.1 degrees) and sensitive ($\lesssim 2\%$ Crab Nebula point-source sensitivity) survey of the Milky Way in very-high-energy γ rays ($0.2 \lesssim E \lesssim 100$ TeV). Roughly ~ 2700 hours of high-quality

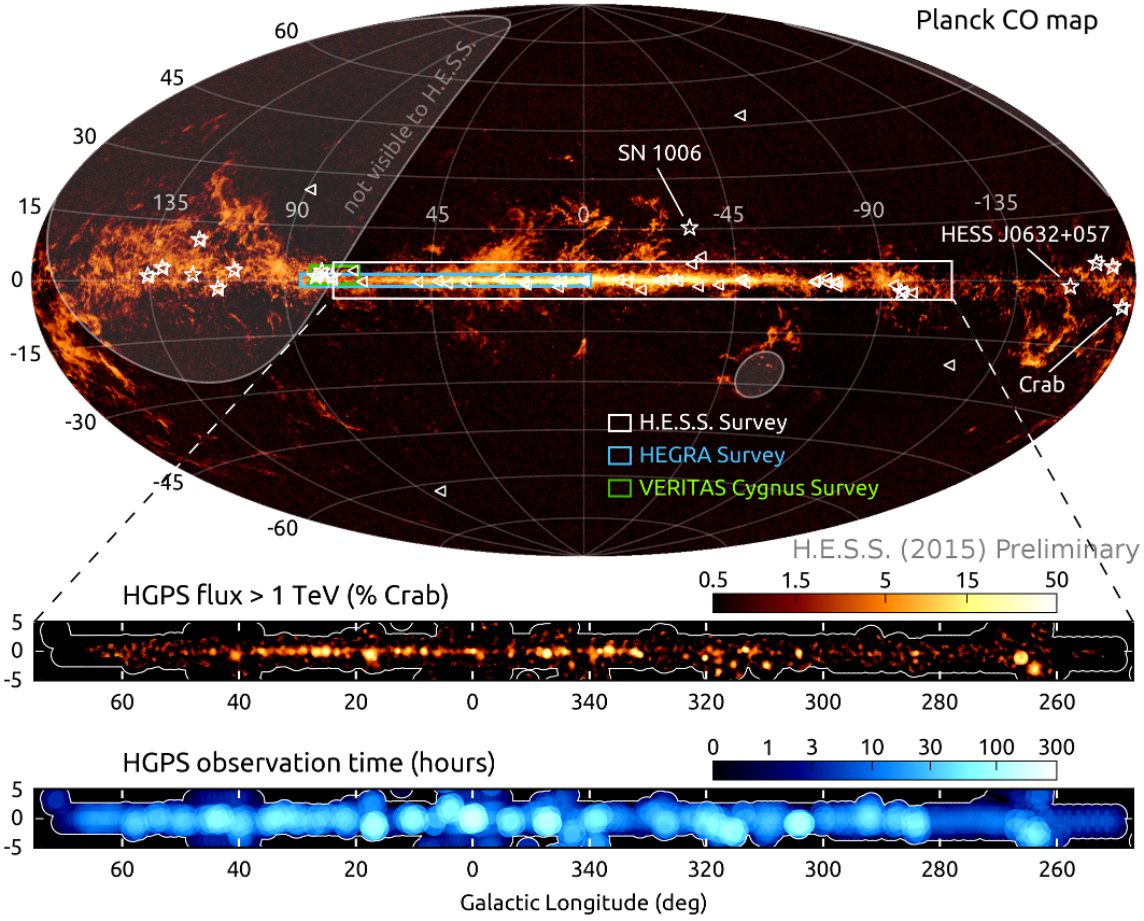

Figure 2: H.E.S.S. Galactic Plane Survey region, flux map and exposure map (from top to bottom). The all-sky image on the top panel shows a Planck CO Map with *Fermi*-LAT identified Galactic 1FHL sources (triangles) and the 15 known Galactic TeV sources (white stars) outside the HGPS region. The HEGRA Galactic Plane Survey [10] and the VERITAS Cygnus survey [11, 12] regions are illustrated in blue and green, respectively. From [13].

observations of the Galactic disk are available in the Galactic longitude range from 250 to 65 degrees and Galactic latitude $|b| < 3.5$ degrees. The region of the Milky Way covered by the HGPS is depicted as a white rectangle in Fig. 2 and compared to the HEGRA (in blue) and VERITAS Cygnus (in green) surveys.

The HGPS data set combines dedicated survey operations (using a fixed-grid pointing strategy) with deep observations of sources of particular interest and follow-up observations of previously discovered sources. Therefore, as shown in Fig. 2, lower panel, the exposure, and thus the sensitivity, is not uniform across the survey region. For the first time, an automatic pipeline was used for source extraction, using a likelihood fit of Gaussian components plus diffuse background. 11 complex sources (e.g. shell supernova remnants) were excluded from the pipeline. A catalogue of 77 cosmic accelerators was obtained, out of which 6 are new sources that were previously unknown or unpublished. A significant fraction of the VHE population are identified as pulsar wind nebulæ (PWN) or supernova remnants (SNR), while the majority remains unidentified or confused.

The HGPS is a unique tool for population studies (e.g. PWN [16] or SNR [17] population studies were shown at the conference). The paper and legacy data will be released soon (Fall 2015), including FITS maps and a source catalog (morphology & spectra) and will certainly become a reference for the community.

2. Supernova Remnants as sources of cosmic rays

Expanding shock waves in SNRs are believed to be able to accelerate cosmic rays up to multi-TeV energies through the mechanism of diffusive shock acceleration (DSA), see e.g. [18]. It was realized very early that, given the rate of ~ 3 explosive events per century, SNRs are capable of maintaining the galactic cosmic ray (CR) flux at the observed level [19], if a fraction of about 10% of their explosion energy is converted into cosmic rays. About 300 SNRs are currently known in the Milky Way, mostly from their non thermal radio emission [20, 21]. Most shell-type SNRs are non-thermal radio emitters, showing evidence that electrons are accelerated up to at least GeV energies. For a recent review of diffusive shock acceleration in the context of SNRs, see e.g. [22].

Several classes of SNRs are potential sites of VHE cosmic-ray acceleration. Composite SNRs host an energetic pulsar at their center, whose non-thermal outflow leads to the formation of a PWN, capable of accelerating electrons up to VHE energies. Young shell-type SNRs are expected to release a significant fraction of their non thermal output at TeV energies, whereas older SNRs, through interactions with clouds of interstellar matter, are more likely to shine at GeV energies, thus allowing the different stages of SNR evolution to be probed using multi-wavelength observations.

In contrast to very high energy electrons, that unavoidably shine in γ rays through inverse-Compton (IC) scattering on cosmological microwave and infrared backgrounds photons, accelerated protons and ions are only revealed when interacting with a dense target, such as a molecular cloud (MC). Electrons, on the other hand, suffer from stronger energy losses and have short live times in dense environments. In the end, the emission mechanism depends more on the environment than on the accelerator itself.

In the last years, SNRs have been firmly established as sources of VHE γ-ray emission. At least five SNRs with clear shell-type morphology resolved in VHE γ rays were detected by H.E.S.S., allowing direct investigation of the SNRs as sources of cosmic rays. They are all rem-

nants of recent supernovae (less than a few kyr): RX J1713.7-3946 [23, 24], RX J0852.04622 (also known as Vela Junior) [25], SN 1006 [26], HESS J1731-347 [27] and RCW 86 [28]. All of them show a very clear correlation between non-thermal X-ray and VHE γ-ray emissions. Recently, two additional candidates of shell-type SNRs were identified in the HGPS [29], HESS J1534-571 and HESS J1912+101, the latter being the first TeV-only shell candidate, identified through its morphology and without known counterpart. Three other shell-type SNRs, Tycho [30, 31], Cas A [32, 33, 34, 35] and IC 443[36, 37] are detected at VHE by MAGIC and VERITAS[1] and at HE [38, 39, 40]. All three exhibit a rather soft spectrum, peaking in the GeV range, and consistent with a pion-bump, thus supporting a hadronic scenario.

2.1 SNR RX J1713.7-3946

The SNR RX J1713.7-3946 is one of the brightest Galactic X-ray SNRs, possibly associated with the guest star AD393 which, according to Chinese astronomers, appeared in the constellation Scorpius [41]. After its discovery by the CANGAROO collaboration [42], It was the first young, shell-type SNR to be resolved in VHE γ rays [23], with a typical shell morphology consistent with X-ray observations.

There is an ongoing debate in the literature about the origin of the emission. Recent observations of RX J1713.7-3946 with the *Fermi*-LAT [43] still suggest that the dominant emission mechanism might be leptonic, although a significant contribution from hadronic cosmic rays cannot be excluded. The lack of X-ray thermal bremsstrahlung emission, predicted in many hadronic scenarios, further support this interpretation [44], as well as the close correlation between the X-ray and γ-ray morphologies. However, γ-ray emission up to 100 TeV is difficult to achieve with IC scattering due to Klein-Nishina suppression of the cross section at high energy. The shape of the high-energy cut off therefore provides a handle on the acceleration mechanism.

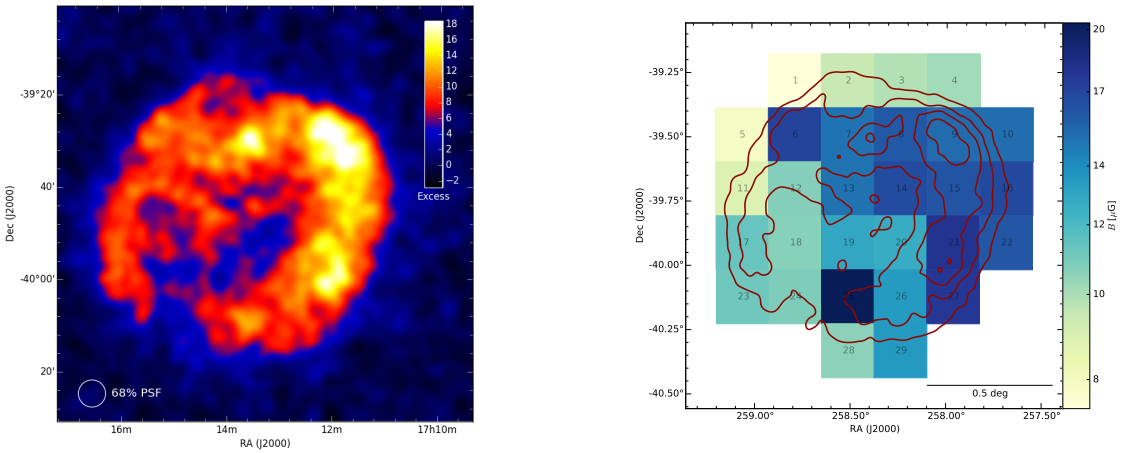

Figure 3: Left: H.E.S.S.VHE γ-ray image of RX J1713.7-3946. **Right**: Map of magnetic field under a leptonic scenario [45].

Under a purely IC scenario for the GeV-TeV spectrum, the model-independent derived electron spectrum exhibits a break at $\sim$ 2 TeV, which could only be obtained with a magnetic field of

[1] Tycho was first discovered by VERITAS, Cas A by HEGRA and IC 443 by MAGIC.

$> 100\ \mu$G, in conflicts with direct estimations. Alternately, a very high photon field energy density (~ 140 eV cm^{-3}) could provide the required target for strong IC emission, but this value exceeds by far recent estimations of the target photon field. In summary, it appears very difficult, given the observational constrains, to explain the *Fermi*-LAT and H.E.S.S. data in a consistent manner, with a purely leptonic model based on a single population of electrons.

Since the last H.E.S.S. publication [24], the amount of data has been doubled. At the same time, high-resolution / high-throughput analysis techniques have been developed, e.g. [46], allowing to spatially resolve spectra with unprecedented resolution ($\lesssim 0.05°$). The resulting γ-ray image is shown in Fig. 3, left, and has an energy threshold of ~ 250 GeV. For the first time, maps of physical quantities, such as magnetic field in the case of a leptonic scenario, can be produced. Fig. 3, right, shows the distribution of magnetic field inside the SNR, inferred from a one-zone leptonic model. In addition, the high statistics collected and the high resolution analysis permits a detailed comparison of the morphology between VHE γ rays and X-rays. The γ-ray image from Fig. 3 has been in five quadrants (Fig. 4, left) for which the radial profiles have been determined. In several regions, such as region 3 (Fig. 4, right) the γ-ray emission appears significantly more extended than the X-ray one (smeared to the H.E.S.S. PSF), indicating for the first time diffusion of particles outside the shell and even escape of high energy particles, most likely of hadronic origin.

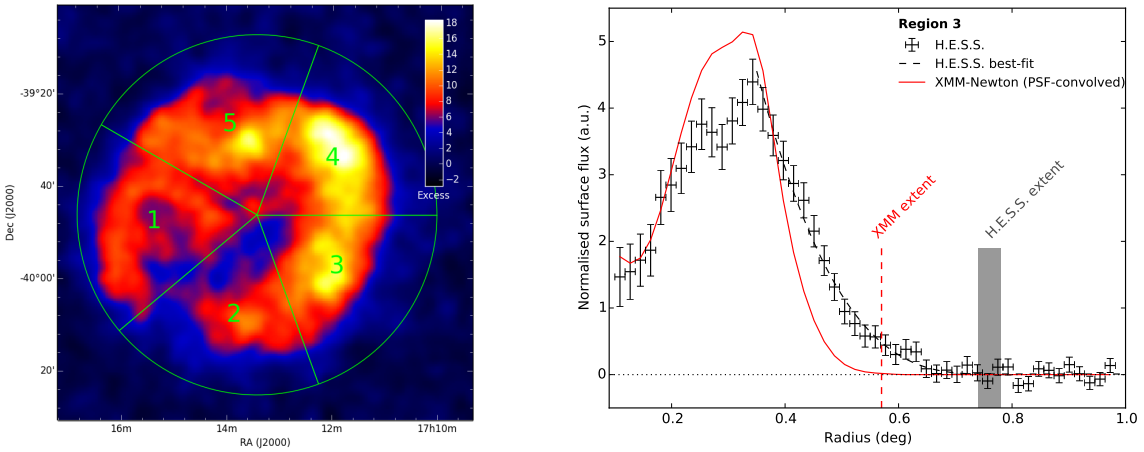

Figure 4: Left: Quadrants used in the H.E.S.S.VHE γ-ray image of RX J1713.7-3946 to investigate possible particle escape. **Right**: Radial profile of γ-ray (black) and X-ray (red) emission in quadrant number 3 [45].

Further studies, and in particular determination of the energy spectrum of escaping particles and detailed investigation of the interaction with the surrounding medium, would further improve our understanding of the underlying acceleration & diffusion mechanisms.

2.2 IC 443

In the GeV domain, the brightest SNRs, IC 443, W44 and W51C are supernovae remnants which interact with MCs, that provide target material for accelerated protons and nuclei. The so-called "*pion bump*", a low energy cutoff in the energy spectrum that clearly indicates emission of γ rays channelled through the decay of neutral pions produced by hadronic interactions, was

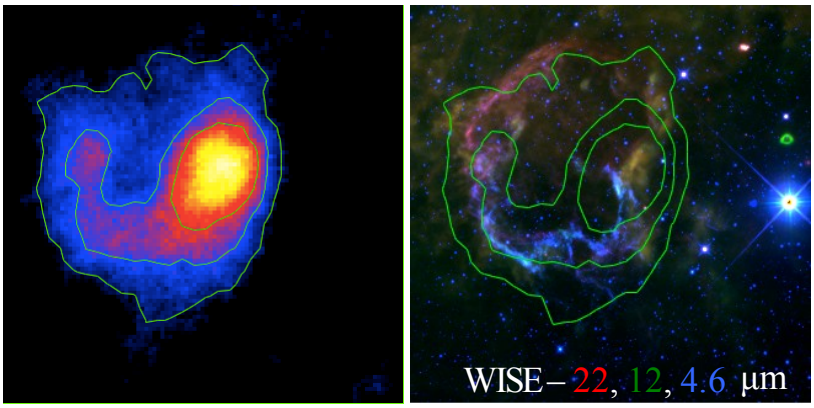

Figure 5: Left: IC 443 shell resolved by VERITAS. **Right**: VERITAS contours superimposed with the Wide-field Infrared Survey Explorer (WISE) map in false colors [50]. WISE image credit: NASA/JPL-Caltech/UCLA

first detected in IC 443 by AGILE [47]. *Fermi*-LAT recently reported its detection in IC 443 & W44 [40].

IC 443, also known as the *Jellyfish Nebula* is a relatively nearby (1.5 kpc) and extended (50' across) SNR, and has been extensively studied for decades. It exhibits a shell-like morphology in optical and in radio [48], consisting of two connected sub-shells with different centers and radii (Fig. 5, right). The complex morphology is attributed to the presence of sharp density gradients and different MCs in the surroundings, e.g. [49], reaching very high density (up to $\sim 10\,000$ cm^{-3}), The latter decelerate the blast wave and affect the expansion of the shell and its morphology.

After initial detection in VHE γ-rays by MAGIC [36] and VERITAS [37], the latter presented for the first time at this conference the shell of IC 443 resolved in γ rays [50]. The corresponding image, superimposed with 3, 6 and 9 σ contours, is shown in Fig. 5, left, and exhibits a clear, shell-like morphology. This will allow for the first time to extract spectra from different regions within the remnant and to probe the environmental dependence of cosmic-ray diffusion. The centroid of the emission is consistent with the emission previously reported by MAGIC and corresponds to the densest part of the MC, where a OH maser emission is also found [51, 52], and where the blast wave is significantly decelerated (Fig. 5, right), thus confirming the hadronic origin of the emission.

3. Gamma-ray binaries: Swiss clocks vs fuzzy clocks

During the last decade, binary systems consisting of a compact object (stellar-mass black hole or neutron star) and a non-degenerate high-mass companion star have been firmly established as VHE γ-ray emitters. To date, five γ-ray binaries, defined as binary systems displaying most of their non-thermal emission at γ-ray energies, have been found. In order of detection, they are: PSR B1259-63 [53], LS 5039 [54], LS I +61° 303 [55], HESS J0632+057 [56] and 1FGL J1018.6-5856 [57]. They exhibit vastly different periods, ranging from few days to several years, and harbour a massive O or Be star with temperature of $20000 - 40000$ K. The orbital period and the companion star mass and temperature of these five γ-ray binaries are summarized in table 1. For an extensive review, see [58] and references therein.

Two main scenarios are currently considered to explain the variable emission from γ-ray binaries (Fig. 6). In the pulsar-wind scenario (left), the system is powered by the wind of a high spin-down power pulsar, that interacts with the wind of the massive star. In the microquasar scenario (right), the system is powered by the accretion of the massive star onto the compact object. Below, we briefly summarize some of the main properties which make γ-ray binaries unique laboratories for high-energy astrophysics:

- They operate in rather extreme environment, with very dense radiation fields and stellar winds, that are not easily found in other systems. These radiation fields can induce strong absorption of γ rays by pair creation on the stellar photons, resulting in a regular modulation given by the periodic changes in the geometry of the system [59, 60].
- The physics at play is complex, both in accretion-based or wind-wind interaction scenarios, with γ rays thought to originate in the interactions with strongly anisotropic radiation fields and/or surrounding material. The conditions, especially in highly eccentric systems, vary significantly along the orbit, resulting in competing effects: acceleration efficiency, energy losses, radiative output and absorption can vary by orders of magnitude, thus producing complex and different phenomenologies. A detailed knowledge of the system geometry is a

	Period (days)	$M_\star(M_\odot)$	$T_\star(K)$
PSR B1259-63	1236	31	33500
LS 5039	3.9	23	39000
LS I +61° 303	26.4	12	22500
HESS J0632+057	315	16	30000
1FGL J1018.6-5856	16.6	31	38900

Table 1: Orbital period and companion star mass and temperature of the five γ-raybinary systems known so far. From [58] and references therein.

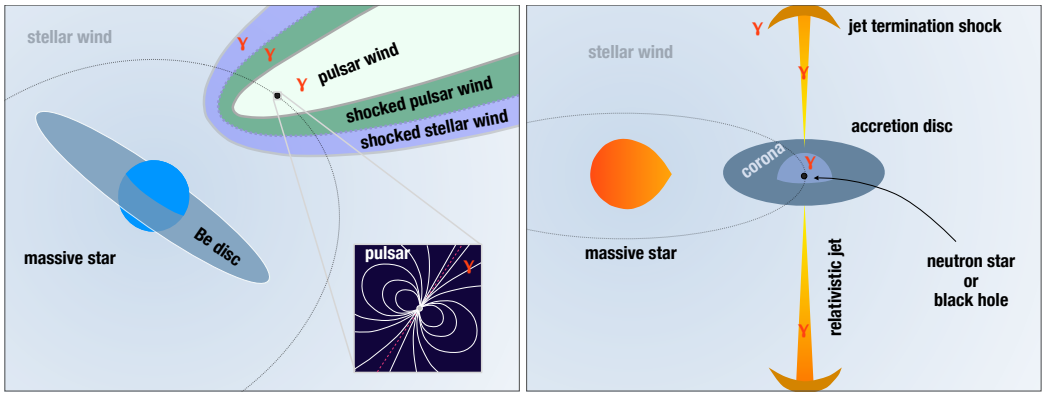

Figure 6: The two main scenarios for γ-ray emission from binaries. **Left**: in the pulsar wind scenario, the variable emission arises from the interaction of the pulsar wind with the strong stellar wind of the companion star. **Right**: in the microquasar scenario, the emission is powered by the accretion of the massive star onto the compact object (black hole or neutron star) giving rise to relativistic jets. Reproduced from [58].

prerequisite for any attempt to understand the emission mechanisms. On the other hand, this offers the unique possibility to test different physical conditions in a single system. In this sense, γ-ray binaries are good laboratories for testing acceleration and radiation/absorption mechanisms.

- The binary nature of the systems allows some of their properties (masses, or at least mass function, inclination, orbit) to be measured with a good precision, allowing rather accurate modelling.

3.1 PSR B1259-63 and LS 5039 - The Swiss clocks

PSR B1259-63 is a long period (3.4 years) binary system in a highly eccentric orbit [53, and references therein]. It is the only γ-ray binary where the nature of the compact object – a pulsar with a spin period of 48 ms – has been firmly established through observations far away from periastron, where the radio pulses are not absorbed by the stellar wind.

Significant γ-ray emission arises only close to periastron, when the pulsar wind interacts with the stellar and circumstellar wind, giving rise to an enhancement of the non-thermal emission visible across the entire electromagnetic spectrum. In addition, the pulsar crosses the circumstellar disk twice, $\sim$ 20 days before and after periastron [61].

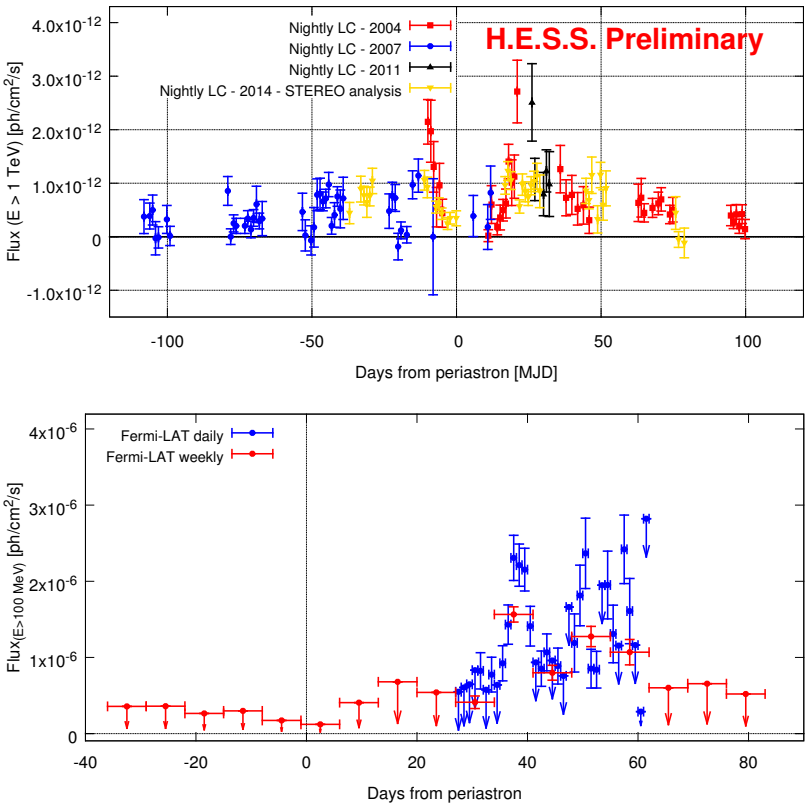

Figure 7: **Top:** H.E.S.S. daily light curves of PSR B1259-63, folded over several periastron passages. **Bottom:** Flux obtained from the analysis of *Fermi*-LAT data in the energy range 100 MeV – 300 GeV. Note that the horizontal scales are different [62].

VHE emission from PSR B1259-63 was first detected by H.E.S.S. during the periastron passage in 2004 [53], and was extensively monitored during the 2007 and 2010/2011 passages [63, 64], whereas the source was not detected during observations far from periastron.

During the 2010/2011 passage, *Fermi*-LAT detected a high energy (HE) flare $\sim$ 30 days after the periastron passage [65]. This flare, without any counterpart at other wavelengths, came as a complete surprise to the community and its nature remains controversial.

Observations with H.E.S.S. during the 2014 periastron passage were reported at the conference [62]. The overall light-curve (Fig. 7, upper panel) is generally consistent with the previous (2004, 2007 and 2010/2011) periastron passages, with, however, some evidence for variability on short time-scales. As in 2010/2011, a strong enhancement of the HE γ-ray flux was measured by *Fermi*-LAT around 30 days after periastron (Fig. 7, lower panel), with a double-peak structure, indicating that this puzzling HE flare is probably a recurrent feature of the system. For the first time, the large H.E.S.S.-II telescope, CT5, was operating during the 2014 periastron passage. No counterpart of the *Fermi*-LAT flare was found in the monoscopic data, down to 200 GeV. However, the source appeared rather bright even $\sim$ 50 days after periastron, displaying a relatively high flux state contemporaneous to the development of the HE flare.

LS 5039 is a compact binary system, with a period of 3.9 days. It has been extensively monitored during the last 10 years by H.E.S.S. [54, 59] and *Fermi*-LAT [66]. A strong modulation of the HE and VHE fluxes with the orbital period, with anti-correlation between the two energy bands, is attributed mainly to anisotropic IC emission and variable absorption of the VHE γ-ray flux by pair creation on stellar photons (the absorption being maximal at the superior conjunction, when the compact object is behind the star) and subsequent production of HE photons by cascading [60].

More recent data [67], including H.E.S.S.-II observations, confirms the perfectly regular behaviour of the source over more than 10 years, and contribute to close the spectral gap between *Fermi*-LAT and H.E.S.S..

3.2 LS I +61° 303 - The fuzzy clock

The binary system LS I +61° 303 is composed of a Be star [68] with a circumstellar disk and an unidentified compact object (neutron star or black hole), in a highly eccentric orbit ($e = 0.54 \pm 0.03$). It was first detected by MAGIC [55] and later on confirmed by VERITAS [69] and *Fermi*-LAT [70]. Although the VHE emission appears to be linked with the orbit (with significant periodicity at VHEs), unlike LS 5039, the orbital phases of VHE detection have varied considerably in different observation campaigns. In early observations, the emission was confined to the phase $0.5 \leq \phi \leq 0.9$ [69, 71, 72]. In observations performed in 2010 the source was instead detected at orbital phases $0 \leq \phi \leq 0.1$ [73].

In addition, the non-thermal emission is characterized by a super-orbital modulation (1667 ± 8 days), detected in radio [74] and HE γ rays [75]. Overall, LS I +61° 303 is an unusual accelerator with rapidly changing conditions. Among the possible explanations for the variability, turbulent mixing of stellar and pulsar winds, a structured stellar wind [76], or the interaction of pulsar winds with stellar disk have been considered.

The exact nature of the system and the underlying emission mechanisms are still subject of debate, with possible scenarios including:

- a pulsar wind scenario, similar to that proposed for LS 5039 and PSR B1259-63, and supported by the detection by VLA of rotating cometary-like structures [77],
- a microquasar scenario, supported by the detection with MERLIN of extended jet-like structures [78],
- finally, after a very short burst (< 0.1 s) detected with Swift, LS I +61° 303 has been proposed to be the first binary system comprising a magnetar [79].

Long-term observations are key to understand the variability of particle acceleration and γ-rayemission in LS I +61° 303. After 8 years of monitoring, VERITAS acquired 160 hours of deep observations of the system. In October 2014, an exceptionally bright ($> 25\%$ of the Crab Nebula flux) and fast ($<$ 1-day rise time) flare was detected by VERITAS [80]. The corresponding light-curve is shown in Fig. 8, left. The system retreated to its quiescent level shortly after, in December 2014. In contrast to the flaring episode of 2007, no significant enhancement was detected at the same time in *Fermi*-LAT, suggesting that different populations of particles might be at the origin of the HE and VHE emissions.

Several mechanisms have been proposed to explain the irregular behaviour of LS I +61° 303. In particular, the so-called *flip-flop* mechanism [79, 82] has been put forward, which relies on a periodic change of the mass-loss rate of the star: close to the periastron, the pulsar magnetosphere is disrupted by the circumstellar wind and the system enters the "*propeller*" regime, characterized by a suppression of the VHE γ-ray emission. At other phases, and in particular around apastron, the usual "*ejector*"' regime applies, with acceleration of particles up to TeV energies in the pulsar magnetosphere. In that scenario, the size of the circumstellar disk would change according to the massive star mass-loss rate. For high mass-loss rate, the "*propeller*" regime could then span the full orbit.

In order to investigate the super-orbital variability of LS I +61° 303, MAGIC performed extended observations between 2010 and 2014 [81]. These, together with the archival data, resulted in the folded light-curve of Fig. 8, right, which is consistent with a sinusoidal variation at the super-

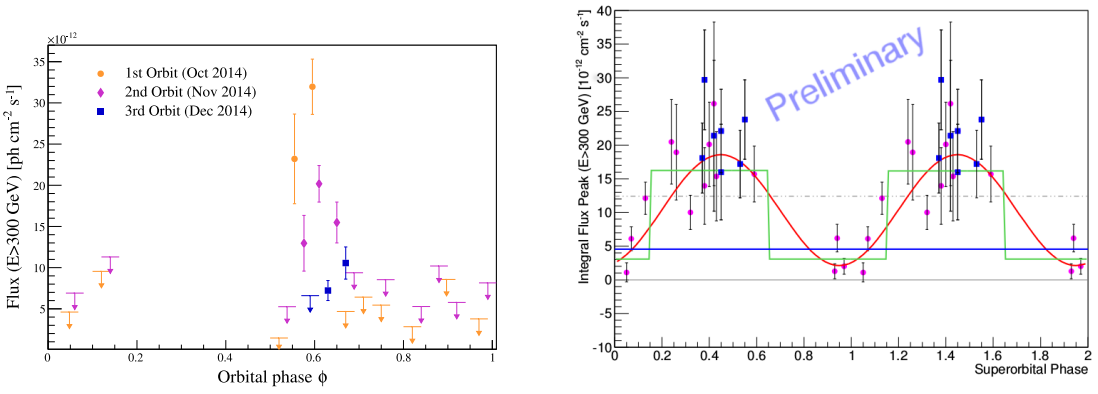
1st Orbit (Oct 2014)
2nd Orbit (Nov 2014)
3rd Orbit (Dec 2014)
Flux (E>300 GeV) [ph cm^{-2} s^{-1}]
Orbital phase ϕ
Preliminary
Integral Flux Peak (E>300 GeV) [10^{-12} cm^{-2} s^{-1}]
Superorbital Phase

Figure 8: Left: VERITAS nightly light curve of LS I +61° 303 during the 2014 observation season [80]. **Right:**MAGIC peak flux of LS I +61° 303 in phase $0.5 - 0.75$, folded with the super-orbital period [81].

orbital phase, and excludes a constant flux. Contemporaneous observations of the H_α line emission with the LIVERPOOL telescope near the MAGIC site could not, however, establish any correlation with the mass-loss rate and the super-orbital phase, leaving the debate still open.

4. Very High Energy pulsars

The first detection of VHE γ-ray pulsed emission above 25 GeV of the Crab pulsar by the MAGIC collaboration [83], and the later detection above 100 GeV [84, 85], triggered an intense theoretical and experimental activity. Energetic pulsars are complex systems, comprising the neutron star itself, its magnetosphere, the ultra-relativistic wind and the PWN surrounding the pulsar (Fig. 9, left).

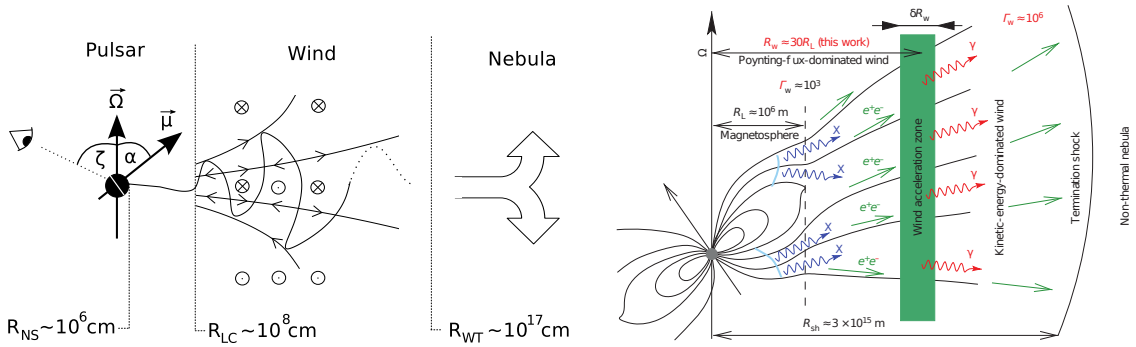

Figure 9: **Left:** Sketch of the components of a PWN. The equatorial current sheet (thick straight line) and the magnetic fields (thin dashed line and circles) are shown in the wind region. Reproduced from [86]. **Right:** Sketch of the different regions surrounding the pulsar, including the magnetosphere, the unshocked wind region and the PWN. In the wind acceleration region (in green), the electromagnetic energy contained in the pulsar wind is converted into bulk kinetic energy of a relativistic e+/e- plasma. Particles are isotropized at the termination shock, and release their energy through synchrotron and IC radiation, resulting in the formation of a non-thermal emitting nebula. Reproduced from [87].

4.1 Crab Pulsar

The Crab Pulsar, PSR B0531+21, is a young energetic pulsar, with a rotation period of ~ 33 ms and a spin-down power of 4.6×10^{38} erg s^{-1}, and is the remnant of the historical supernova in 1054 A.D. Being relatively nearby (~ 2 kpc), it is one of the most studied non-thermal astronomical sources. Pulsed HE γ-ray emission was already detected by EGRET [88], triggering an intense and successful search for pulsed emission in VHE γ rays:

- 2008: First detection of pulsed emission above 25 GeV by the MAGIC collaboration [83]
- 2011: First detection of pulsed emission in the $120-400$ GeV energy range by the VERITAS collaboration. Pulsed emission in this energy range was theoretically rather unexpected and started to challenge existing pulsar models. The VHE emission appeared to originate from a new, power-law component, possibly extending to even higher energies. In order to avoid strong energy losses of high energy electrons by synchrotron radiation, these γ rays must be produced more than 10 stellar radii away from the neutron star [84].

- 2011: First spectrum in the $25-100$ GeV energy range by MAGIC [89].
- 2012: Spectrum extending to 400 GeV by MAGIC [85]
- 2014: Detection of VHE emission from the bridge between the two peaks P1 and P2 at energies ≥ 50 GeV by MAGIC [90]

The detection of VHE pulsed emission of the Crab Pulsar triggered a lot of theoretical activity. Several models have been proposed, all of them placing the emission far away from the neutron star, close to the light cylinder or even beyond. In the Annular Gap model for instance [93], the gap region is located between the critical field lines and the last open field lines, possibly extending up to the light cylinder. As for the outer gap [94] or slot gap models [95], VHE emission arises from IC up-scattering of lower energy photons, see e.g. [89]. VHE γ-ray emission could also be produced in the striped wind of the pulsar, from IC scattering of pulsed X-ray photons [96, 87, 97] (Fig. 9, right). For a recent review of existing models, see for instance [86].

Both the VERITAS and MAGIC collaborations have devoted a large amount of observation time (respectively 195 and 320 hours) to further investigate the energy extension of the emission and evolution of pulse shape with energy, for better constraining the existing emission models. The phasograms of the Crab Pulsar obtained by the MAGIC and VERITAS collaborations are shown in Fig. 10 [91, 92]. Both of them reported the detection of P1 and P2 peaks in the $100-400$ GeV energy domain at a high significance level. Above 400 GeV, only MAGIC detects the two peaks, whereas the combined excess counts from P1 and P2 yields only $2\,\sigma$ for VERITAS. MAGIC reported at this conference pulsed emission up to approximately 2 TeV, which requires a parent population of electrons with a Lorentz factor of at least 5×10^6. Above 950 GeV, 119 ± 54 and

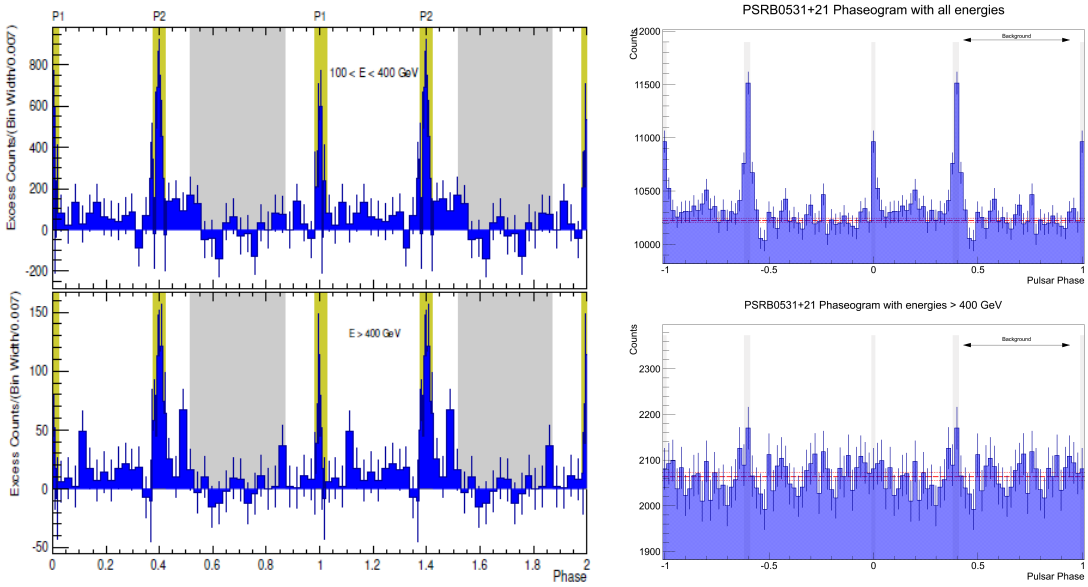

Figure 10: Phase-folded distribution of events from the Crab Pulsar("*phasogram*"). **Left:** MAGIC results in the $100-400$ GeV energy domain (top) and >400 GeV (bottom) [91]. **Right:** VERITAS results for all energies (top) and >400 GeV (bottom) [92].

190 ± 56 excess events are detected in pulses P1 and P2 respectively, corresponding to significances of 2.2 and $3.5\,\sigma$ [98]. This exciting discovery further challenges pulsar models, with VHE γ-ray emission likely to take place in the neighbourhood of the light cylinder ($r \sim 1600$ km). VERITAS could not yet confirm this important discovery. Nevertheless, further observation extending up to 300 hours have been planned by the VERITAS collaboration to extend results to higher energies.

MAGIC also recently reported the detection of emission from the bridge between P1 and P2 above 50 GeV, with a statistical significance of $6.2\,\sigma$ [90]. Although qualitative explanations of the bridge can be found, for instance in [99], a consistent picture of the VHE Crab pulsed emission is still lacking further theoretical developments.

4.2 Vela Pulsar

Despite its longer period, $P = 89.3$ ms, compared to the Crab pulsar, its larger characteristic age $\tau_c = 11$ kyr and its much smaller spin-down power $\dot{E} = 6.9 \times 10^{36}$ erg s^{-1} [100], the Vela pulsar is, due to its proximity ($d = 287^{+19}_{-17}$ pc [101]) exceptionally bright in radio and in HE γ rays, and is, after the Crab pulsar, one of the best natural candidates for VHE emission. The Vela pulsar is surrounded by a strong wind nebulae, detected in particular by *Fermi*-LAT [102].

The HE γ-ray phasogram is characterized by two main sharp peaks (P1 and P2) and a third peak (P3) in the bridge (Fig. 11, bottom). The ratio of the peak intensity between P1 and P2, and the location and intensity of P3 vary with energy [104, 105].

Various models are able to properly describe the HE γ-ray emission of the Vela pulsar. For instance, in the framework of the annular model, e.g. [106], curvature radiation of primary particles

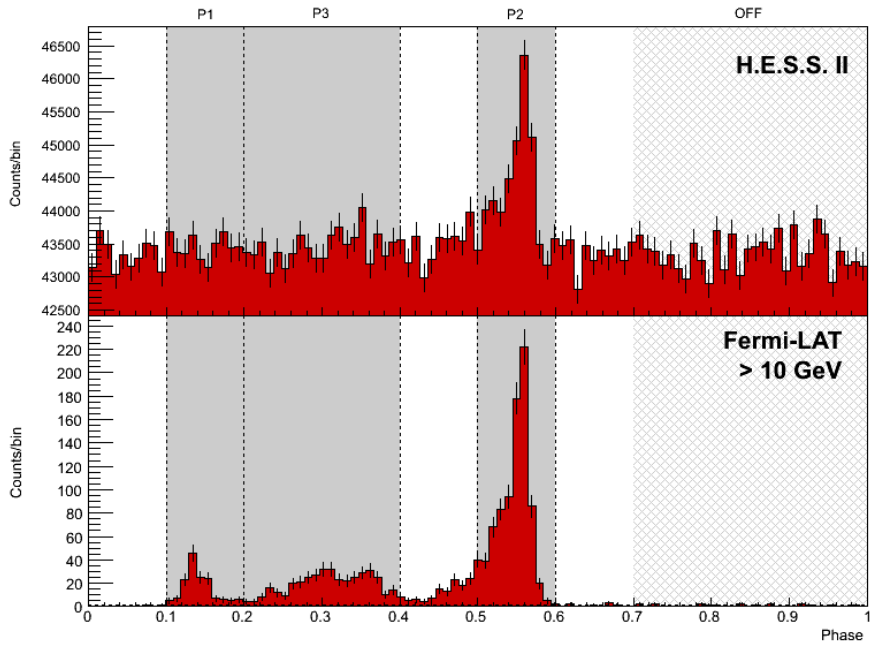

Figure 11: Phase-folded distribution of events of the Vela Pulsar with H.E.S.S.-II (top) and *Fermi*-LAT(bottom) [103].

is responsible for the emission, without the need of curvature radiation from secondary particles nor IC scattering.

The pulsed flux component does however fall very quickly with energy, and the lack of statistics with the *Fermi*-LAT does not allow the shape of the cut-off to be constrained, nor the presence of another component at higher energies, possibly similar to that observed in the Crab pulsar, to be identified. H.E.S.S.-II, with is much larger effective area ($\sim 10^4$ m^2 at 20 GeV) and low energy threshold, is perfectly suited to the observation of VHE pulsars. 24 hours of high quality data were obtained by H.E.S.S.-II in 2013 and 2014, and were analyzed with a dedicated set of analysis cuts, leading to a very low energy threshold ($\sim$ 20 GeV).

The phased-folded event distribution obtained is shown in Fig. 11, top. Nearly 10 000 excess events were detected in the pulse P2, corresponding to a Li & Ma significance of 12.8 σ. No significant excess is observed from the P1 peak, nor from the P3, which is in agreement with an extrapolation of the *Fermi*-LAT phasogram.

The energy distribution (Fig. 12, left) of the reconstructed events from P2 is fully compatible with expectations from Monte Carlo (MC) simulations (power law with spectrum index -4.1), and indicates that H.E.S.S.-II is able to detect γ rays with energy as low as 10 GeV, although with a significant reconstruction energy bias. A preliminary spectral energy distribution between 20 and 120 GeV (Fig. 12, right) is consistent with extrapolations from the *Fermi*-LAT measurement, but the available statistics and systematic uncertainties, still under study, limit the possibility to discriminate between different shapes of the high energy cut-off, as well as to establish a possible new component at very high energies.

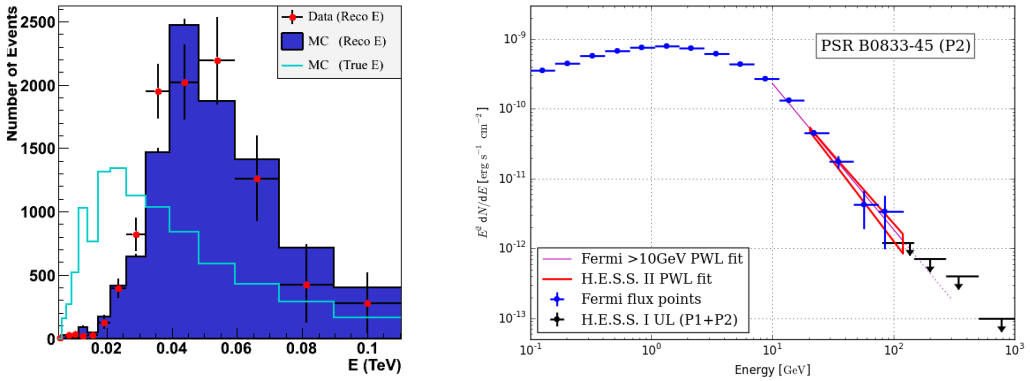

Figure 12: Left: Reconstructed energy distribution of the excess events in P2 peak (red points) compared to the prediction of a Monte Carlo simulation (dark blue histogram). The corresponding true energy distribution for the MC (light blue) indicates that H.E.S.S.-II is able to detect γ rays with energy as low as 10 GeV. **Right:** Spectral energy distribution of the P2 peak of Vela with *Fermi*-LAT and H.E.S.S.-II [103].

5. Powerful Stellar-like emitters in the LMC

The Large Magellanic Cloud (LMC) is a satellite galaxy of the Milky Way, situated at 50 kpc from the Earth with a size of $\sim 10^\circ$ in the sky (corresponding to an intrinsic size of 8 kpc). Host

of the last nearby supernova (SN 1987A [107]), it has been subject of extensive monitoring campaigns during the last years, in particular to investigate how fast young SNRs can start accelerating particles to very high energies. The LMC is also a somewhat extreme laboratory for the study of particle accelerators, due to very large cosmic ray and radiation densities, as well as intense star formation activity and supernova rate (larger by a factor of ~ 8 than in the Milky Way [108]). It also contains the best example of a local starburst, the Tarantula Nebula (30 Doradus), the largest star-forming region in the Local Group of galaxies.

In 2010 *Fermi*-LAT published [111] the detection of large-scale diffuse emission, attributed to the interaction of cosmic rays with the interstellar medium, but could not resolve any single source in the LMC. The HE γ-ray emission appears to exhibit a much closer correlation with star forming regions than with interstellar gas, suggesting a relatively short GeV cosmic-ray proton diffusion length compared to that in the Milky Way.

The H.E.S.S. collaboration accumulated, over the last years, a deep exposure of 210 hours on the LMC, targeted at the Tarantula nebula. Sophisticated analysis techniques were used to improve the angular resolution of the instrument and resolve the different sources. Three sources of different types were detected, all of them having some peculiar characteristics (Fig. 13):

- N157 B, already detected with a smaller data set [112], is a PWN associated with the most powerful pulsar known so far (PSR J0537-6910, spin-down power $\dot{E} = 4.9 \times 10^{38}$ erg s^{-1} [86]). Despite a rather low acceleration efficiency and low inferred magnetic field (~ 45 μG), it is

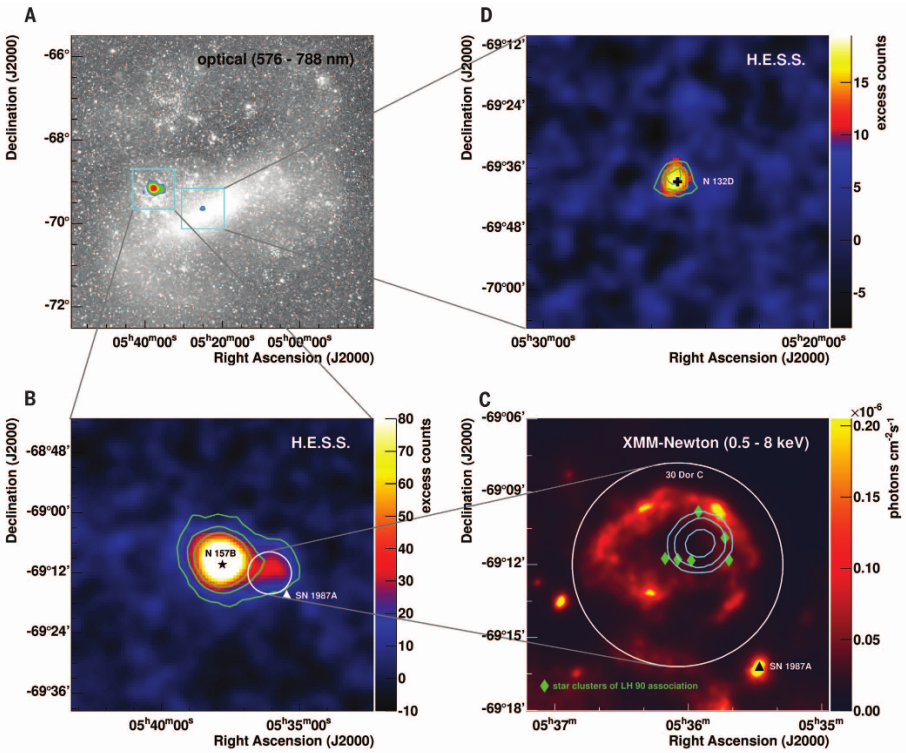

Figure 13: Powerful emitters in the LMC as seen by H.E.S.S. and XMM-Newton [109, 110]

ten times brighter in TeV γ rays than the Crab Nebula, most likely due to the very high surrounding target radiation fields.

- N 132D is a particularly old, γ-ray emitting, radio-loud SNR, possibly interacting with dense, shocked interstellar clouds. A hadronic emission scenario would imply a very high energy in protons ($\sim 10^{52}$ erg), 10 times larger than for archetypal young SNRs in the Galaxy such as Cas A. With an age of $\sim$ 6000 yrs [113], between GeV and TeV emitting SNRs, it allows probing the time span during which the SNRs are able to accelerate particles to tens of TeV energies.

- The superbubble 30 Dor C is the first unambiguous detection of a superbubble in VHE γ rays. 30 Dor C is, with a radius of 47 pc, the largest non thermal, X-ray shell known so far [114], filled with hot gas and likely blown into the interstellar medium by multiple supernovae and stellar winds. The TeV luminosity of 30 Dor C implies extreme conditions, both for a leptonic or a hadronic scenario, and supports the hypothesis that superbubbles might be able to accelerate particles above 10^{15} eV.

Last but not least, the unique object SN 1987A is, despite theoretical prediction (e.g. [115]), not detected, which constrains the theoretical framework of particle acceleration in very young SNRs. For first time individual, stellar-like, cosmic-ray accelerators are identified in an external galaxy. For the first time as well, superbubbles are firmly identified as sources of VHE γ rays.

6. Peculiar extragalactic objects

Active Galactic Nuclei, consisting of an accreting supermassive black hole associated with large scale, non-thermal jets, are among the most powerful non-thermal sources in the Universe. In *blazars*, having one of the jets pointing at the direction of the Earth, the Doppler boosted non-thermal output from the jet completely outshines the host galaxy. Their emission is characterized by strong outbursts ("*flares*") and fast variability, sometimes down to time scales of minutes.

In the last years, the number of VHE extragalactic sources has been growing steadily, the vast majority of the newly discovered sources belonging to this class of blazars. Several blazar discoveries and results from multi-wavelength monitoring campaigns have been presented at the conference. Among others, the H.E.S.S. collaboration presented the first H.E.S.S.-II results, in monoscopic mode, on the well know high synchrotron peaked objects PKS 2155-304 and PG 1553+113 [116]. The data acquired with CT5 revealed a significant spectral curvature for both sources with respect to a simple power-law spectrum and contributed to close the gap with *Fermi*-LAT.

A few AGNs exhibit particularly interesting characteristics and will be described in the following.

6.1 IC 310 Lightning from a Black Hole

IC 310 is a nearby ($z = 0.0189$) radio galaxy, located in the outskirts of the Perseus cluster of Galaxies, and hosting a $3 \times 10^8 M_\odot$ super-massive black hole [117]. It shows a broad-band non-thermal emission, detected from the radio to the VHE γ rays [118]. IC 310 was originally classified as a head-tail radio galaxy. Recent Very Long Baseline Interferometry (VLBI) established the

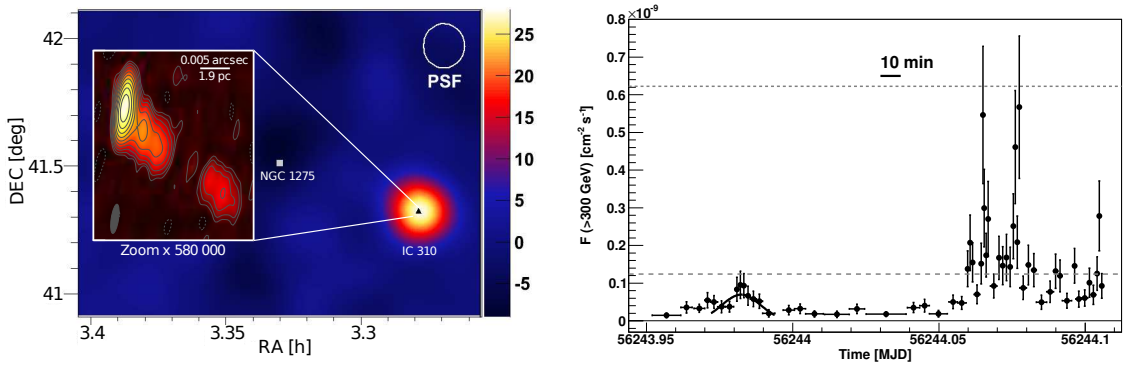

Figure 14: Left: Combined image of the significance map measured by MAGIC above 300 GeV of the Perseus cluster of galaxies and the radio map obtained from EVN observations [119]. **Right:** Light curve above 300 GeV of the flare recorded by MAGIC in 2012 [117, 121].

existence of straight jets, showing the same direction from parsec to kiloparsec [119], and revealed a blazar-like inner jet with a missing counter jet (Fig. 14, left). From these observations, IC 310 was classified as a peculiar object in-between blazars and radio galaxies, with an angle between the jet-axis and the line-of-sight measured to be $10^\circ \lesssim \theta \lesssim 20^\circ$ [120]. This was further supported by the measurement of low Doppler factors in the jets with radio telescopes [119].

During a multi-wavelength campaign organized by the MAGIC collaboration in 2012, an exceptionally bright VHE flare was detected, reaching the flux of the Crab Nebula above 1 TeV and showing very fast variability, down to timescales of a few minutes (Fig. 14, right). Due to the non-zero angle of the jet, the variability timescale cannot be significantly lowered by Doppler boosting, and therefore allows the size of the emission region to be constrained to be smaller than 20% of the Schwarzschild radius of the central black hole. In frequently used AGN models, such as the so-called *shock-in-jet* model, such small emission regions would unavoidably result in strong absorption of VHE γ-ray emission by pair creation on the synchrotron radiation ("*opacity*" argument).

New models have been proposed to circumvent the opacity problem, see [117] and references therein, including mini-jet structures within the jets, jet-cloud/star interactions, and magnetospheric models [122]. The latter, inspired from pulsar models, is able to reproduce the main features of the VHE γ-ray emission. In this model, the black hole is assumed to spin maximally. A particle-starved magnetosphere is then anchored to the ergosphere (location at which space-time is flowing at the speed of light), leading to the formation of vacuum gaps where electrons and positrons can be accelerated to ultrahigh energies. Theses develop electromagnetic cascades, multiplying the number of charge carriers, until the induced current shortcuts the gap. This analysis however relies almost completely on the measured jet angle. For a smaller jet angle ($\theta \lesssim 5^\circ$), usual shock-in-jet models would probably be able to reproduce the observed features.

6.2 Quasar half-way to the edge of the observable Universe

PKS 1441+25 is an flat spectrum radio quasar (FSRQ) located at a red-shift of $z = 0.939$. First detected in VHEs by MAGIC [123] at a statistical significance of $25\,\sigma$ after a MeV-GeV flare [124], it was quickly confirmed by VERITAS [125] (at a statistical significance of $\sim 8\,\sigma$).

The source appeared to be steady at that time, at ∼ 5% of the Crab flux above 80 GeV with a very soft spectrum. In later observations in May 2015, after the end of the MeV-GeV flare, PKS 1441+25 could not be detected at the same level in VHEs. Being one of the two most distant VHE blazar ever, the source is of particular interest. Detected up to ∼ 250 GeV, it implies important constraints on the extragalactic background light (EBL) [126, 127]. With five detected objects only so far, FSRQs currently form only a small fraction of the VHE extragalactic sources.

6.3 QSO B0218+357: A Gravitationally lensed blazar

Due to the strong absorption of VHE γ rays by pair creation on the EBL, most of VHE blazars known so far are relatively close-by, with red-shift $z \lesssim 0.5$. Below 100 GeV, where the sensitivity of IACTs start somewhat degrading, the observable Universe extends to $z \sim 1$.

QSO B0218+357 is a distant blazar, likely a flat spectrum radio quasar, located at the red-shift of $z = 0.944$ [128] and gravitationally lensed by the galaxy B0218+357 G located at the red-shift of 0.68. Einstein's rings separated by only 335 mas have been detected in radio [129]. Time delays between the two components have been detected in radio (of $10-12$ days) [130] and recently in HE γ rays (11.46 ± 0.16 days), using auto-correlation analysis of the light curve [131].

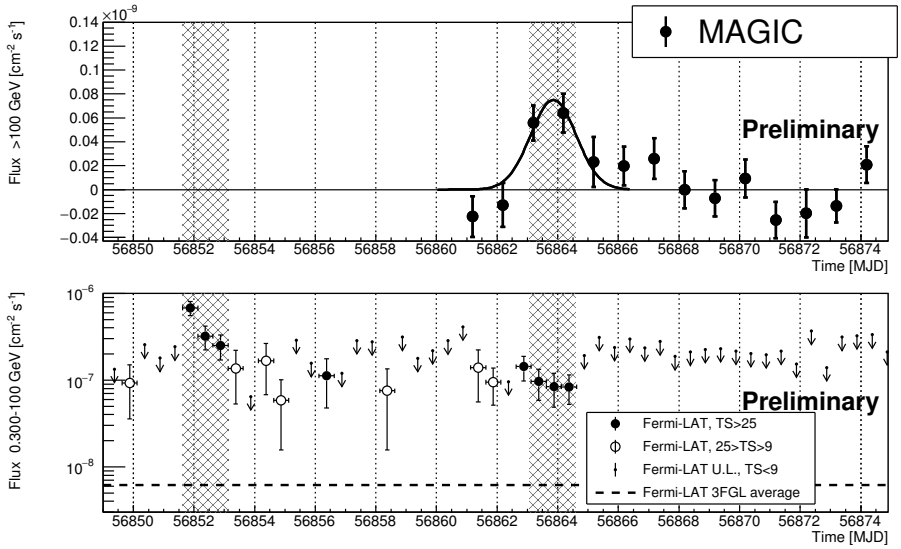

Figure 15: The gravitationally lensed blazar QSO B0218+357. **Top:** MAGIC nightly light curve above 100 GeV. **Bottom:** *Fermi*-LAT light curve above 0.3 GeV [132]

In July 2014, QSO B0218+357 entered a flaring state in HE [133], with an intensity increase by a factor of ∼ 20. Due to full moon period, MAGIC could not detect the original HE flare, but detected the source at the expected arrival time of the delayed flare [134], with a statistical significance of $5.7\,\sigma$. The corresponding *Fermi*-LAT and MAGIC light curves are shown in Fig. 15.

QSO B0218+357 is, with PKS 1441+25 one of the two most distant sources (red-shift $z \sim 0.9$) known in VHE γ rays, allowing to derive strong constrains on the EBL.

PKS 1830-211, another gravitationally lensed blazar, was observed with H.E.S.S.-II in August 2014 following an alert issued by the *Fermi*-LAT collaboration on a flaring state, to search for a

potential VHE counterpart in active state with a delay of $\sim$ 20 days as detected with *Fermi*-LAT in a previous flare from this source [135]. No detection were achieved based on 8.6 h of data, leaving thus QSO B0218+357 as the only gravitationally lensed blazar detected at the VHE energies.

6.4 Distant sources & EBL measurement

The VHE energy spectrum of distant AGNs is affected by pair creation on the EBL and on the CMB. The imprint depends on the energy and on the red-shift of the source. Several probes can be used to obtain constrains on the EBL:

- Single sources at large distance, such as PKS 1441-25 or 1ES 1101+496 can be used to derive upper limits of the EBL density.

- Measurement of several sources at different distances allow, under some assumption of the intrinsic spectrum, to measure the EBL density at different distances. This has been done recently [136] using 86 spectra from 38 individual VHE sources, corresponding to a total of $\sim 270,000$ γ rays. Using a sophisticated statistical treatment, evidence of the imprint of γ-rayabsorption is found at the 11 σ significance level in the energy spectra of VHE blazars. The reconstructed EBL spectrum is in good agreement with estimates based on galaxy counts (below direct measurements), and leaves room for contributions from e.g. intra-halo light. Several results presented at the conference supported this conclusion [127, 137, 126].

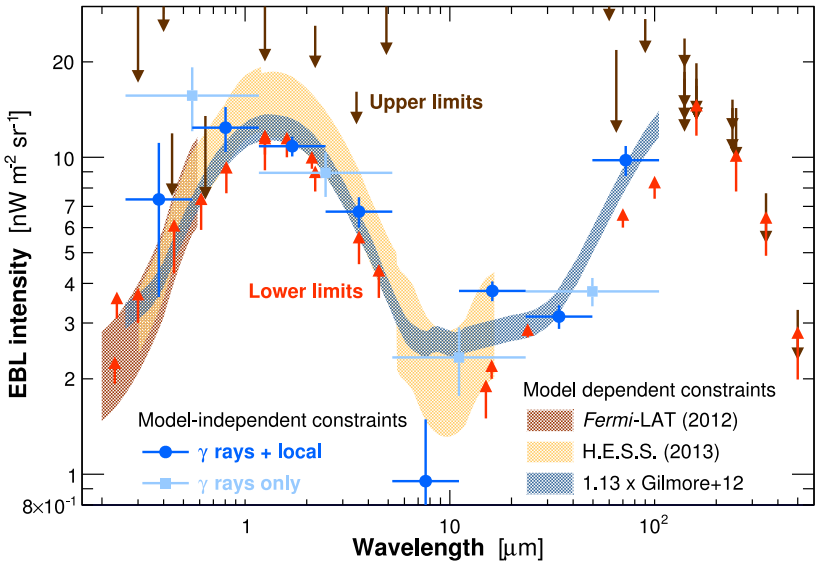

Figure 16: Local EBL measurement using a large sample of VHE blazars [136].

Conclusions and perspectives

Nearly 10 years after the coming in of the third generation instruments, the field of ground based γ-ray astronomy is still very active. Numerous technical developments, together with elaborated analysis techniques, have resulted in major improvements of the sensitivity of the instruments (Fig.1). This translated almost directly into the number of detected sources at VHEs, as shown in the current VHE catalogue (Fig. 17). The number of discoveries as function of time is shown in Fig. 18. Similarly to the evolution of the X-ray domain in the 1960's, there is almost an exponential rise of the number of sources, without any saturation so far. For many researchers, the recent success of VHE astronomy comes as a surprise, as in the 1980's only a handful of them believed there was any detectable γ-raysource above 100 GeV.

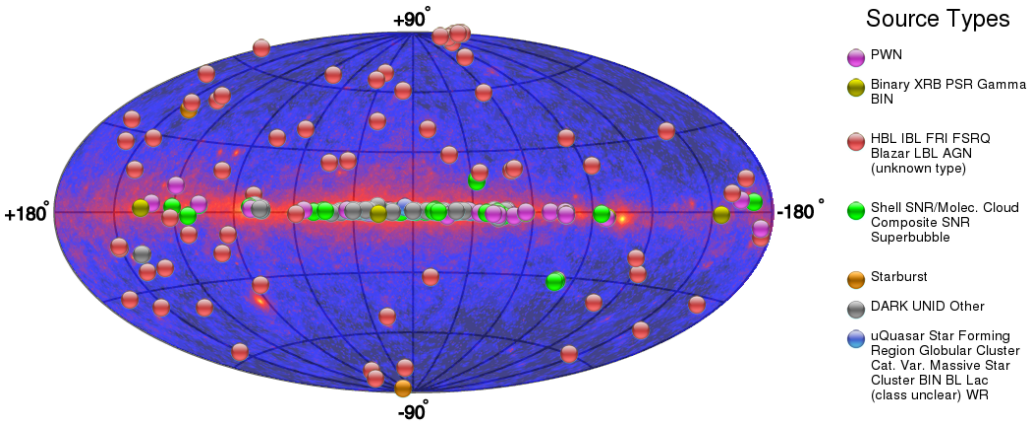
+90°
+180°
-180°
-90°
Source Types
PWN
Binary XRB PSR Gamma BIN
HBL IBL FRI FSRQ Blazar LBL AGN (unknown type)
Shell SNR/Molec. Cloud Composite SNR Superbubble
Starburst
DARK UNID Other
uQuasar Star Forming Region Globular Cluster Cat. Var. Massive Star Cluster BIN BL Lac (class unclear) WR

Figure 17: Current catalogue of VHE sources. From http://tevcat.uchicago.edu/.

The field is however experiencing a phase transition, as most of the brightest sources are probably already detected. Large surveys and deep exposures of specific sources are now defining the general trend. At the same time, large multi-wavelength observation campaigns, involving many different observatories operating across the electromagnetic spectrum, proved to be the most effective way to unveil the nature of the very high energy variable sources. With the advent of the Cerenkov Telescope Array (CTA), this will most likely be more and more the case. A reorganization of the collaborations, similar to that of optical observatories, is unavoidable. Open calls for observation proposals and data rights either partially or completely public will probably become the next paradigm.

Despite the numerous successes of VHE ground based astronomy, some important results are still awaited:

- Dark matter, predicted in many theories to annihilate in pairs of high energy γ grays, has not been detected so far. Recent limits from Dwarf Galaxies are becoming very constraining.
- Despite huge efforts to improve the relocation speed and the energy threshold of the telescopes and to minimize the dead time between consecutive observations, and despite evidence from *Fermi*-LAT of emission up to $\sim$ 100 GeV [138], still Gamma Ray Bursts (GRBs) remain undetected at VHEs [139].

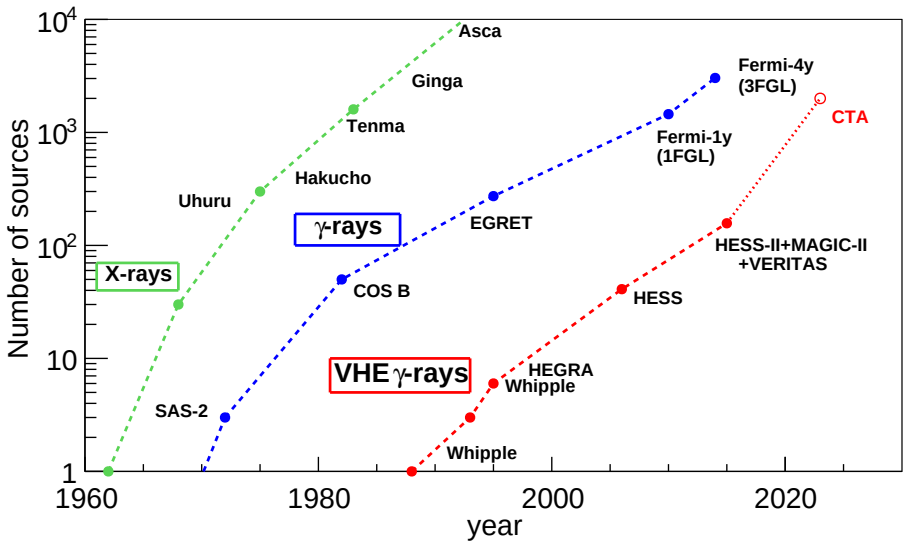

Figure 18: The so-called Kifune plot showing evolution of number of sources at different wavelengths as a function of time and different instruments [1].

- Definite proof of acceleration of hadrons, though the detection of very high energy neutrinos from astrophysical sources, are still missing.
- Sources of Ultra High Energy cosmic rays, above 10^{15} eV, are still unidentified. SNRs are commonly thought to be able to accelerate cosmic rays up to the knee, however no *Pevatron* has been firmly identified yet.

With an improvement by a factor of ~ 10 in sensitivity, and with a significantly better angular resolution, CTA [140] will be the next breakthrough in VHE ground based γ-ray astronomy. Construction phase should begin in 2016 with the goal to operate the full array by 2021. Exciting discoveries are still ahead of us.

Acknowledgements

The author is very grateful to the H.E.S.S., MAGIC and VERITAS collaborations for providing their results. He would like to thank in particular Reshmi Mukherjee and Razmik Mirzoyan for very interesting and fruitful discussions.

References

[1] de Naurois, M. & Mazin, D., C. r. Acad. sci., *in press* (2015) .
[2] Staszak, D. V. C., in: PoS(ICRC2015) 868, (2015).
[3] Park, N. V. C., in: PoS(ICRC2015) 771, (2015).
[4] Giavitto, G., Ashton, T., Balzer, A., et al., in: PoS(ICRC2015) 771, (2015).
[5] Atkins, R., Benbow, W., Berley, D., et al., ApJ, 608 (2004) 680–685.
[6] Abdo, A. A., Allen, B., Berley, D., et al., ApJL, 664 (2007) L91–L94.
[7] Abeysekara, A. U., Aguilar, J. A., Aguilar, S., et al., Astropart. Phys., 35 (2012) 641–650.
[8] Abeysekara, A. U., Alfaro, R., Alvarez, C., et al., Astropart. Phys., 50 (2013) 26–32.
[9] Pretz, J. H. C., in: PoS(ICRC2015) 866, (2015).
[10] Aharonian, F. A., Akhperjanian, A. G., Beilicke, M., et al., A&A, 395 (2002) 803–811.
[11] Weinstein, A. & for the VERITAS Collaboration, ArXiv e-prints (2009) .
[12] Popkow, A. V. C., in: PoS(ICRC2015) 750, (2015).
[13] Deil, C., Brun, F., Carrigan, S., et al., in: PoS(ICRC2015) 773, (2015).
[14] Aharonian, F., Akhperjanian, A. G., Aye, K., et al., Science, 307 (2005) 1938.
[15] Aharonian, F., Akhperjanian, A. G., Bazer-Bachi, A. R., et al., ApJ, 636 (2006) 777.
[16] Klepser, S. H. C., in: PoS(ICRC2015) 777, (2015).
[17] Hahn, J., Fernandez, D., Casanova, ., et al., in: PoS(ICRC2015) 860, (2015).
[18] Drury, L. O., Reports on Progress in Physics, 46 (1983) 973–1027.
[19] Baade, W. & Zwicky, F., Proceedings of the National Academy of Science, 20 (1934) 259–263.
[20] Green, D. A., Bulletin of the Astronomical Society of India, 32 (2004) 335–370.
[21] Ferrand, G. & Safi-Harb, S., Advances in Space Research, in press (2012) .
[22] Hillas, A. M., Journal of Physics G Nuclear Physics, 31 (2005) 95–+.
[23] Aharonian, F. A., Akhperjanian, A. G., Aye, K., et al., Nature, 432 (2004) 75–77.
[24] Aharonian, F., Akhperjanian, A. G., Bazer-Bachi, A. R., et al., A&A, 464 (2007) 235–243.
[25] Aharonian, F., Akhperjanian, A. G., Bazer-Bachi, A. R., et al., A&A, 437 (2005) L7–L10.
[26] Acero, F., Aharonian, F., Akhperjanian, A. G., et al., A&A, 516 (2010) A62+.
[27] Acero, F., Pühlhofer, G., Klochkov, D., et al., in: PoS(ICRC2013), (2009).
[28] Aharonian, F., Akhperjanian, A. G., de Almeida, U. B., et al., ApJ, 692 (2009) 1500–1505.
[29] Pühlhofer, G., Brun, F., Capasso, M., et al., in: PoS(ICRC2015) 886, (2015).
[30] Acciari, V. A., Aliu, E., Arlen, T., et al., ApJL, 730 (2011) L20.
[31] Park, N. V. C., in: PoS(ICRC2015) 769, (2015).
[32] Aharonian, F., Akhperjanian, A., Barrio, J., et al., A&A, 370 (2001) 112–120.
[33] Albert, J., Aliu, E., Anderhub, H., et al., A&A, 474 (2007) 937–940.
[34] Acciari, V. A., Aliu, E., Arlen, T., et al., ApJ, 714 (2010) 163–169.
[35] Kumar, S. V. C., in: PoS(ICRC2015) 760, (2015).
[36] Albert, J., Aliu, E., Anderhub, H., et al., ApJL, 664 (2007) L87–L90.
[37] Acciari, V. A., Aliu, E., Arlen, T., et al., ApJL, 698 (2009) L133–L137.
[38] Giordano, F., Naumann-Godo, M., Ballet, J., et al., ApJL, 744 (2012) L2.
[39] Abdo, A. A., Ackermann, M., Ajello, M., et al., ApJL, 710 (2010) L92–L97.
[40] Ackermann, M., Ajello, M., Allafort, A., et al., Science, 339 (2013) 807–811.
[41] Wang, Z. R., Qu, Q.-Y., & Chen, Y., A&A, 318 (1997) L59–L61.
[42] Enomoto, R., Tanimori, T., Naito, T., et al., Nature, 416 (2002) 823–826.
[43] Abdo, A. A., Ackermann, M., Ajello, M., et al., ApJ, 734 (2011) 28.
[44] Ellison, D. C., Patnaude, D. J., Slane, P., & Raymond, J., ApJ, 712 (2010) 287–293.
[45] Eger, P., Parsons, R. D., Berge, D., et al., in: PoS(ICRC2015) 766, (2015).
[46] de Naurois, M. & Rolland, L., Astropart. Phys., 32 (2009) 231–252.

[47] Tavani, M., Giuliani, A., Chen, A. W., et al., ApJL, 710 (2010) L151–L155.
[48] Braun, R. & Strom, R. G., A&A, 164 (1986) 193–207.
[49] Cornett, R. H., Chin, G., & Knapp, G. R., A&A, 54 (1977) 889–894.
[50] Humensky, B. V. C., in: PoS(ICRC2015) 875, (2015).
[51] Claussen, M. J., Frail, D. A., Goss, W. M., & Gaume, R. A., ApJ, 489 (1997) 143–159.
[52] Hewitt, J. W., Yusef-Zadeh, F., Wardle, M., Roberts, D. A., & Kassim, N. E., ApJ, 652 (2006) 1288–1296.
[53] Aharonian, F., Akhperjanian, A. G., Aye, K., et al., A&A, 442 (2005) 1.
[54] Aharonian, F., Akhperjanian, A. G., Aye, K., et al., Science, 309 (2005) 746–749.
[55] Albert, J., Aliu, E., Anderhub, H., et al., Science, 312 (2006) 1771.
[56] Aharonian, F. A., Akhperjanian, A. G., Bazer-Bachi, A. R., et al., A&A, 469 (2007) L1.
[57] Ackermann, M., Ajello, M., Ballet, J., & et al., Science, 335 (2012) 189.
[58] Dubus, G., A&AR, 21 (2013) 64.
[59] Aharonian, F., Akhperjanian, A. G., Bazer-Bachi, A. R., et al., A&A, 460 (2006) 743.
[60] Dubus, G., Cerutti, B., & Henri, G., A&A, 477 (2008) 691–700.
[61] Chernyakova, M., Abdo, A. A., Neronov, A., et al., MNRAS, 439 (2014) 432–445.
[62] Romoli, C., Bordas, P., Mariaud, C., et al., in: PoS(ICRC2015) 873, (2015).
[63] Aharonian, F., Akhperjanian, A. G., Anton, G., et al., A&A, 507 (2009) 389.
[64] H.E.S.S. Collaboration, Abramowski, A., Acero, F., et al., A&A, 551 (2013) A94.
[65] Abdo, A. A., Ackermann, M., Ajello, M., et al., ApJL, 736 (2011) L11.
[66] Abdo, A. A., Ackermann, M., Ajello, M., et al., ApJL, 706 (2009) L56–L61.
[67] Mariaud, C., Bordas, P., Aharonian, F., et al., in: PoS(ICRC2015) 885, (2015).
[68] Hutchings, J. B. & Crampton, D., PASP, 93 (1981) 486–489.
[69] Acciari, V. A., Beilicke, M., Blaylock, G., et al., ApJ, 679 (2008) 1427–1432.
[70] Abdo, A. A., Ackermann, M., Ajello, M., et al., ApJL, 701 (2009) L123–L128.
[71] Acciari, V. A., Aliu, E., Arlen, T., et al., ApJ, 700 (2009) 1034–1041.
[72] Albert, J., Aliu, E., Anderhub, H., et al., ApJ, 693 (2009) 303–310.
[73] Acciari, V. A., Aliu, E., Arlen, T., et al., ApJ, 738 (2011) 3.
[74] Gregory, P. C., ApJ, 575 (2002) 427–434.
[75] Ackermann, M., Ajello, M., Ballet, J., et al., ApJL, 773 (2013) L35.
[76] Paredes-Fortuny, X., Bosch-Ramon, V., Perucho, M., & Ribó, M., A&A, 574 (2015) A77.
[77] Dhawan, V., Mioduszewski, A., & Rupen, M., in: VI Microquasar Workshop, (2006).
[78] Massi, M., Ribó, M., Paredes, J. M., et al., A&A, 414 (2004) L1–L4.
[79] Torres, D. F., Rea, N., Esposito, P., et al., ApJ, 744 (2012) 106.
[80] O'Faoláin de Bhróithe, A. V. C., in: PoS(ICRC2015) 781, (2015).
[81] Fernández-Barral, A., Blanch, O., de Oña Wilhelmi, E., et al., in: PoS(ICRC2015) 732, (2015).
[82] Li, J., Torres, D. F., Zhang, S., et al., ApJL, 744 (2012) L13.
[83] Aliu, E., Anderhub, H., Antonelli, L. A., et al., Science, 322 (2008) 1221–.
[84] VERITAS Collaboration, Aliu, E., Arlen, T., et al., Science, 334 (2011) 69–.
[85] Aleksić, J., Alvarez, E. A., Antonelli, L. A., et al., A&A, 540 (2012) A69.
[86] Bühler, R. & Blandford, R., Reports on Progress in Physics, 77 (6) (2014) 066901.
[87] Aharonian, F. A., Bogovalov, S. V., & Khangulyan, D., Nature, 482 (2012) 507–509.
[88] Nolan, P. L., Fierro, J. M., Lin, Y. C., et al., A&AS, 120 (1996) C61.
[89] Aleksić, J., Alvarez, E. A., Antonelli, L. A., et al., ApJ, 742 (2011) 43.
[90] Aleksić, J., Ansoldi, S., Antonelli, L. A., et al., A&A, 565 (2014) L12.
[91] de Oña Wilhelmi, E., Zanin, R., Carreto Fidalgo, D., et al., in: PoS(ICRC2015) 746, (2015).
[92] Nguyen, T. J. V. C., in: PoS(ICRC2015) 828, (2015).
[93] Du, Y. J., Qiao, G. J., & Wang, W., ApJ, 748 (2012) 84.

[94] Venter, C., Johnson, T. J., & Harding, A. K., ApJ, 744 (2012) 34.
[95] Harding, A. K., Stern, J. V., Dyks, J., & Frackowiak, M., ApJ, 680 (2008) 1378–1393.
[96] Bogovalov, S. V. & Aharonian, F. A., MNRAS, 313 (2000) 504–514.
[97] Pétri, J., MNRAS, 424 (2012) 2023–2027.
[98] Aleksić, J., Ansoldi, S., Antonelli, L. A., et al., A&A, *submitted* (2015) .
[99] Bednarek, W., MNRAS, 424 (2012) 2079–2085.
[100] Manchester, R. N., Hobbs, G. B., Teoh, A., & Hobbs, M., AJ, 129 (2005) 1993–2006.
[101] Dodson, R., Legge, D., Reynolds, J. E., & McCulloch, P. M., ApJ, 596 (2003) 1137–1141.
[102] Abdo, A. A., Ackermann, M., Ajello, M., et al., ApJ, 713 (2010) 146–153.
[103] Gajdus, M., Djannati-Ataï, A., Chrétien, M., et al., in: PoS(ICRC2015) 841, (2015).
[104] Abdo, A. A., Ackermann, M., Ajello, M., et al., ApJ, 713 (2010) 154–165.
[105] Abdo, A. A., Ackermann, M., Ajello, M., et al., ApJS, 187 (2010) 460–494.
[106] Du, Y. J., Han, J. L., Qiao, G. J., & Chou, C. K., ApJ, 731 (2011) 2.
[107] Arnett, W. D., Bahcall, J. N., Kirshner, R. P., & Woosley, S. E., ARA&A, 27 (1989) 629–700.
[108] Harris, J. & Zaritsky, D., AJ, 138 (2009) 1243–1260.
[109] H.E.S.S. Collaboration, Abramowski, A., Aharonian, F., et al., Science, 347 (2015) 406–412.
[110] Komin, N., Lu, C., Mayer, M., et al., in: PoS(ICRC2015) 849, (2015).
[111] Abdo, A. A., Ackermann, M., Ajello, M., et al., A&A, 512 (2010) A7.
[112] H.E.S.S. Collaboration, Abramowski, A., Acero, F., et al., A&A, 545 (2012) L2.
[113] Hughes, J. P., Hayashi, I., & Koyama, K., ApJ, 505 (1998) 732–748.
[114] Bamba, A., Ueno, M., Nakajima, H., & Koyama, K., ApJ, 602 (2004) 257–263.
[115] Berezhko, E. G., Ksenofontov, L. T., & Völk, H. J., ApJ, 732 (2011) 58.
[116] Zaborov, D., Romoli, C., Taylor, A. M., et al., in: PoS(ICRC2015) 808, (2015).
[117] Aleksić, J., Ansoldi, S., Antonelli, L. A., et al., Science, 346 (2014) 1080–1084.
[118] Aleksić, J., Antonelli, L. A., Antoranz, P., et al., ApJL, 723 (2010) L207–L212.
[119] Kadler, M., Eisenacher, D., Ros, E., et al., A&A, 538 (2012) L1.
[120] Aleksić, J., Antonelli, L. A., Antoranz, P., et al., A&A, 563 (2014) A91.
[121] Glawion, D. E., Sitarek, J., Mannheim, K., et al., in: PoS(ICRC2015) 729, (2015).
[122] Levinson, A. & Rieger, F., ApJ, 730 (2011) 123.
[123] Mirzoyan, R., in: The Astronomer's Telegram # 7416, (2015).
[124] Pacciani, L., in: The Astronomer's Telegram # 7402, (2015).
[125] Mukherjee, R., in: The Astronomer's Telegram # 7433, (2015).
[126] Becerra González, J., Lindfors, E., Prandini, E., et al., in: PoS(ICRC2015) 876, (2015).
[127] Benbow, W. V. C., in: PoS(ICRC2015) 821, (2015).
[128] Linford, J. D., Taylor, G. B., Romani, R. W., et al., ApJ, 744 (2012) 177.
[129] O'Dea, C. P., Baum, S. A., Stanghellini, C., et al., AJ, 104 (1992) 1320–1330.
[130] Biggs, A. D., Browne, I. W. A., Helbig, P., et al., MNRAS, 304 (1999) 349–358.
[131] Cheung, C. C., Larsson, S., Scargle, J. D., et al., ApJL, 782 (2014) L14.
[132] Sitarek, J., Becerra González, J., Dominis Prester, D., et al., in: PoS(ICRC2015) 825, (2015).
[133] Buson, S. & Cheung, C. C., in: The Astronomer's Telegram # 6316, (2014).
[134] Mirzoyan, R., in: The Astronomer's Telegram # 6349, (2014).
[135] Abdo, A. A., Ackermann, M., Ajello, M., et al., ApJ, 799 (2015) 143.
[136] Biteau, J. & Williams, D. A., ApJ, *in press* (2015) .
[137] Mirzoyan, R. M. C., in: PoS(ICRC2015) 889, (2015).
[138] Ackermann, M., Ajello, M., Asano, K., et al., Science, 343 (2014) 42–47.
[139] Carosi, A., Antonelli, L. A., Becerra GonzÃąlez, J., et al., in: PoS(ICRC2015) 809, (2015).
[140] Acharya, B. S., Actis, M., Aghajani, T., et al., Astropart. Phys., 43 (2013) 3–18.